L- and *M*-electron populations of fast xenon ions traveling in gases

V. Horvat, R. L. Watson, and J. M. Blackadar
Cyclotron Institute and Department of Chemistry, Texas A&M University, College Station, Texas 77843
(Received 15 August 1997)

Spectra of L x rays emitted by 5.2- to 14.4-MeV/nucleon Xe ions traveling in gaseous targets of He, Ne, and Ar have been measured with a curved crystal spectrometer. Detailed spectral analysis provided estimates of the average projectile charges and the average L- and M-electron populations *inside* the gases. In comparisons of the present results for gases with those obtained previously for solids, it was found that Xe ions emitting L x rays in solids have, on average, many more L vacancies than those that emit L x rays in gases. Average charges deduced for Xe ions traveling in Ar gas were 2.3 units lower than the average charges of Xe ions traveling in solid KCl. [S1050-2947(98)08605-3]

PACS number(s): 34.50.Fa, 32.30.Rj

I. INTRODUCTION

It has long been known that energetic heavy ions traveling in gases emerge with lower average charges than those that characterize the equilibrium charge distributions of ions emerging from solids. This observation is qualitatively consistent with ideas that evolved out of the early work on stopping powers by Bohr and Lindhard [1]. In a gas, the average time between collisions that excite or ionize inner-shell electrons of a projectile ion is generally long compared to the time required for relaxation back to the ground state, whereas in the high density environment of a solid, the collision frequency may be shorter than inner-shell relaxation times. Therefore, inner-shell electrons are expected to be more vulnerable to ionization via multiple collisions in solids than they are in gases.

The validity of the above explanation was brought into question by early measurements of heavy ion stopping powers (dE/dx), which failed to find any significant differences between the dE/dx values for gases and solids [2,3]. Consequently, Betz and Grodzins were led to argue that, while the states of excitation may be appreciably different, the effective charges inside gases and solids are essentially the same [4]. According to their model, the enhanced charges exhibited by ions emerging from solid targets result from additional electron loss outside the target via the Auger decay of inner-shell vacancies. Because of the low collision frequency in gases, very few ions are expected to emerge from gas targets with inner-shell vacancies and, hence, this would explain why the charges of ions emerging from solids are larger than the charges of ions emerging from gases.

Over the years, several attempts at determining the charges of ions *inside* solids have been reported [5,6], and the results of these measurements have clearly shown that, under certain conditions, Auger decay indeed does cause the charges of ions emerging from solids to increase by several units over those that exist inside. In more recent times, however, new stopping power measurements have revealed a significant gas-solid effect in which gas stopping powers are observed to be systematically lower than those observed for solid media [7–11]. The effect is found to be largest for high Z_1 projectiles and low Z_2 targets. Thus, it now appears that there is some truth in both points of view.

The inner-shell vacancy states of fast ions traveling in matter can be characterized by examination of the x rays they emit. Therefore, x-ray spectral measurements provide a potential means of investigating the effects of target density on the distribution of inner-shell vacancy states. Moreover, x-ray energies are sensitive to the number of outer-shell electrons attached to the projectile and, hence, they also furnish information concerning the charges of ions *inside* the target medium. In a recent study of L x-ray emission by 6- to 15-MeV/nucleon Xe ions traveling in solids, methods were developed for estimating projectile L- and M-shell electron populations from L x-ray spectra [12,13]. It was shown that under suitable conditions, reliable estimates of the ionic charges of projectiles in solid targets can be obtained by this technique. In an effort to compare the states of fast Xe ions traveling in gases and solids, similar measurements have been performed on a variety of gas targets and the same analysis methods applied to the determination of electron populations and ionic charges. The results of this study are presented herein, and they provide further (independent) verification that the charges of ions traveling in gases are substantially lower than those of ions traveling in solids.

II. EXPERIMENTAL METHODS

Beams of 6-, 8-, 10-, and 15-MeV/nucleon Xe with initial charges ranging from 17+ (6 MeV/nucleon) to 25+ (15 MeV/nucleon) were extracted from the Texas A&M K-500 superconducting cyclotron, charge analyzed, and optically focused on a Zn/CdS phosphor with the aid of a closed-circuit television camera. The beam passed through a 2 mm diam collimator located directly in front of the target gas cell and its intensity was monitored by measuring the current generated in a Faraday cup positioned directly behind the exit window of the gas cell.

The beam entrance and exit apertures of the gas cell were sealed from the vacuum system by means of 2.1 mg/cm^2 nickel foils. This closed-cell design enabled spectral measurements to be performed with targets of He, Ne, and Ar at pressures up to 1 atm. While most of the spectra were taken at a nominal pressure of 700 Torr, measurements investigating the pressure dependence of Xe L x-ray emission in a Ne

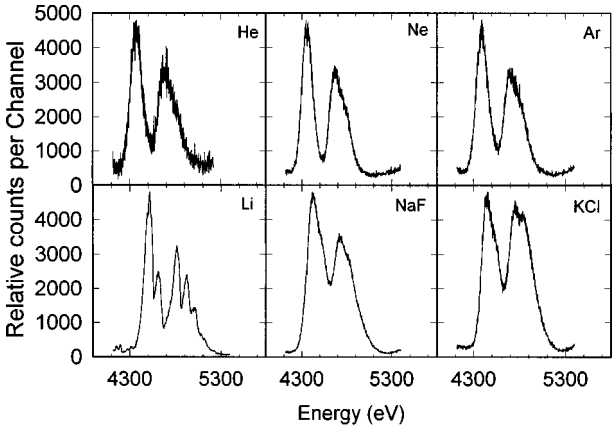

FIG. 1. Spectra of L x rays emitted by 5.2-MeV/nucleon Xe ions traveling in the indicated gases (top panels) and the indicated solids (bottom panels).

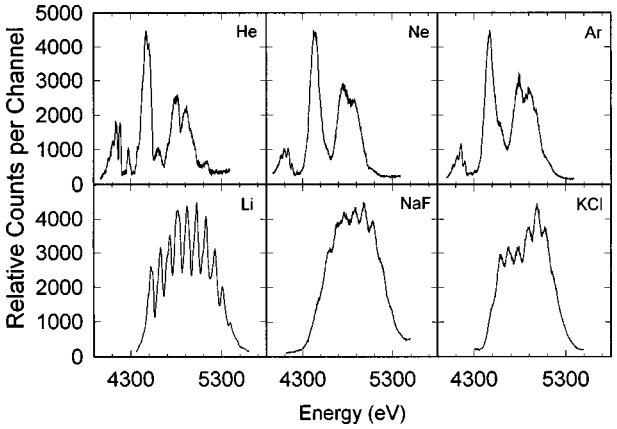

FIG. 3. Spectra of L x rays emitted by 9.3-MeV/nucleon Xe ions traveling in the indicated gases (top panels) and the indicated solids (bottom panels).

target were pursued down to 50 Torr. The first Ni gas cell window caused the beam to enter the gas cell with the equilibrium charge distribution of a slightly lower energy beam emerging from a solid. The average energy of the Xe projectiles (in MeV/nucleon) after passing through the Ni window was reduced to 5.2 (from 6.0), 7.2 (from 8.0), 9.3 (from 10.0), and 14.4 (from 15.0). The distance between the entrance and exit apertures was 1.5 cm and the x rays were viewed through a 540 μg/cm^2 mylar window at the top of the cell. A collimator placed over the x-ray window restricted the projectile path length viewed by the spectrometer to 0.33 cm.

A 12.7-cm Johansson-type curved-crystal spectrometer with the focal circle oriented perpendicular to the beam axis was used to record the Xe L x-ray spectra. Energy calibration of the x-ray spectrometer was performed using the measured diffraction positions of the $K\alpha_{1,2}$ and $K\beta_1$ peaks fluoresced in solid targets containing K, Ca, and Mn, as well as the $L\alpha_{1,2}$ peak fluoresced in a Xe gas target. It was found that the position of the $L\alpha_{1,2}$ peak of Xe agreed quite well with the calibration curve defined by the other reference peaks, verifying that the geometric conditions were the same for both solid and gas targets. The energy calibration was checked several times during the course of each run. The spectrometer had a resolution of 17 eV (FWHM) at an energy of 5000 eV. Further details concerning the gas cell, spectrometer, and the electronic apparatus are given in Refs. [12,14].

III. RESULTS AND DISCUSSION

A. Qualitative features of the spectra

Spectra obtained in the current investigation using He, Ne, and Ar gas targets are compared with those obtained previously [13] using Li, NaF, and KCl solid targets in Figs. 1–4. They reveal that the average electron configurations are quite different for Xe projectiles traveling in gases and solids. The structural features in the solid-target Xe L x-ray spectra are due primarily to overlapping sets of $L\alpha$, $L\beta_1$, and $L\beta_3$ peaks from initial state configurations involving different numbers of L electrons. For example, the spectrum for a Li target (at an incident projectile energy of 5.2 MeV/nucleon) in Fig. 1 displays two $L\alpha$ peaks in the energy range 4300–4700 eV—one arising from single L-vacancy configurations and the other from double L-vacancy configurations. The structure in the energy range 4700–5300 eV is due to the $L\beta$ peaks from these same L-vacancy configurations. It

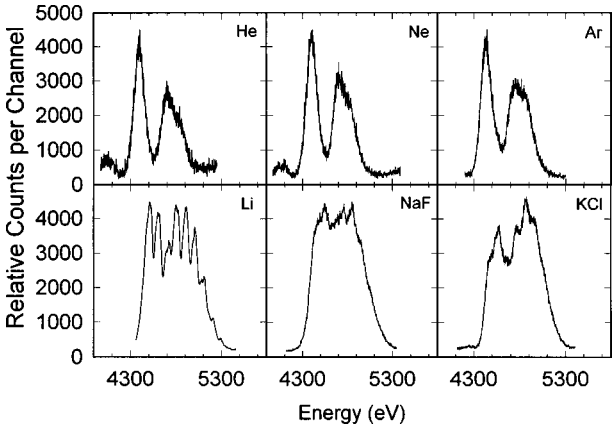

FIG. 2. Spectra of L x rays emitted by 7.2-MeV/nucleon Xe ions traveling in the indicated gases (top panels) and the indicated solids (bottom panels).

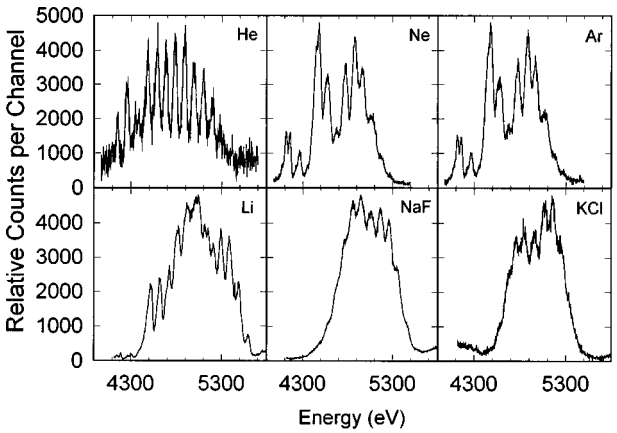

FIG. 4. Spectra of L x rays emitted by 14.4-MeV/nucleon Xe ions traveling in the indicated gases (top panels) and the indicated solids (bottom panels).

is evident that basically the same structural features are present in the spectrum for a NaF target in Fig. 1, but in this case the peaks are much broader than those in the spectrum for a Li target. The reason for this is that, on average, the Xe ions traveling in Li have only 1.2 M electrons, while those traveling in NaF have 5.9 [12]. Each missing M electron causes the L x-ray peaks to shift up in energy by approximately 24 eV and variations in their number give rise to the observed broadening. The gas target spectra shown in Fig. 1 all look quite similar and they contain very little contribution from double L-vacancy configurations.

The spectra for an incident projectile energy of 7.2 MeV/nucleon (Fig. 2) reveal that multiple ionization of the L shell increases rapidly with increasing projectile energy in the solid targets (e.g., the triple L-vacancy $L\alpha$ peak is clearly visible in the spectrum for a Li target). The spectra for the gas targets, on the other hand, look almost the same as those in Fig. 1. Upon closer inspection, however, it becomes evident that the peaks are slightly shifted to higher energies, indicating that fewer M electrons are present.

At an incident projectile energy of 9.3 MeV/nucleon (Fig. 3), the peaks in the gas-target spectra are somewhat narrower than at the lower projectile energies, indicating that many more of the M electrons have been removed, and the double-L-vacancy $L\alpha$ peak has become visible, especially in the He spectrum where it is clearly resolved. Also, a set of unidentified peaks (centered around 4100 eV) have become rather prominent. These mysterious peaks appear in all of the spectra for gas targets at projectile energies above 7.2 MeV/nucleon. Moreover, their structure appears to depend on the state of ionization of the projectile, as can be seen by comparing the spectra obtained with gas targets in Figs. 3 and 4. They also are observed in spectra obtained with thick Li targets and with thin targets (see Fig. 3 of Ref. [12]) at all of the projectile energies investigated, although their intensities are greatly reduced relative to the $L\alpha$ peaks. These peaks do not appear in any of the other spectra for thick solid targets. This last observation may indicate that they originate from metastable states that, because of their relatively long lifetimes, are highly quenched in the high density environment of a solid.

The spectrum for a He target undergoes a remarkable transformation in going from an incident projectile energy of 9.3 MeV/nucleon (Fig. 3) to 14.4 MeV/nucleon (Fig. 4). In the latter case, the peaks are very narrow and there are substantial contributions from electron configurations with as many as four L vacancies. Another interesting point is that if the unidentified peaks (below 4400 eV in Fig. 4) are excluded, this spectrum closely resembles the spectrum for a Li target at 9.3 MeV/nucleon (Fig. 3). The 14.4 MeV/nucleon spectra for Ne and Ar targets are almost identical. They display observable contributions from electron configurations having up to three L vacancies, and their structure closely resembles that displayed by the spectra for Li targets at 5.2 and 7.2 MeV/nucleon.

As the Xe ions emerged from the Ni gas cell entrance window and traveled to the spectrometer observation region, they adjusted to a new charge distribution characteristic of the gas. Since the target thickness required to reach a new equilibrium distribution is not known, it was necessary to check to see if the L x-ray spectra were pressure dependent.

TABLE I. Average projectile L- and M-electron populations ($\overline{n_L}$ and $\overline{n_M}$), average projectile charges ($\overline{Q}$), and charge distributions widths (σ_Q) determined from least-squares fitting analysis of the spectra of L x rays emitted by Xe ions traveling in gases. The estimated uncertainties are ± 0.4 for $\overline{n_L}$ and $\overline{n_M}$, and ± 0.6 for $\overline{Q}$.

Incident projectile energy (MeV/nucleon)	Target	$\overline{n_L}$	$\overline{n_M}$	$\overline{Q}$	σ_Q
5.2	He	7.0	7.5	37.5	2.1
	Ne	7.0	8.1	36.9	2.1
	Ar	7.0	6.6	38.4	2.0
7.2	He	6.9	6.3	38.8	2.1
	Ne	6.9	6.1	39.0	2.1
	Ar	6.8	4.8	40.4	2.0
9.3	He	6.9	1.6	43.5	1.2
	Ne	6.9	4.0	41.1	1.8
	Ar	6.7	2.5	42.8	1.7
14.4	He	5.4	1.0	45.6	1.6
	Ne	6.4	1.3	44.3	1.3
	Ar	6.3	1.3	44.4	1.3

Spectra were measured for 14.4 MeV/nucleon Xe ions in Ne at pressures of 50, 100, and 700 Torr (equivalent target thicknesses of 41, 81, and 570 μg/cm^2, respectively). The L x-ray spectra at all of these pressures looked nearly identical to the one in Fig. 4 and, hence, it was concluded that even the L x-ray spectrum obtained with a He target at 700 Torr (equivalent thickness of 113 μg/cm^2) was representative of a fully equilibrated beam.

B. Quantitative analysis of the spectra

The spectra obtained in the present investigation were analyzed using the fitting procedure described in [13]. Since the projectile energies in the gas targets were well defined, the application of Doppler shift corrections was straightforward, in contrast to the problems encountered with thick solid targets of low atomic number in which the x rays are observable over a wide range of projectile energies as they slow down in the target. The results of this analysis are given in Table I. Estimates of the average charges rely on the assumption that all shells above the M shell are empty. This assumption is quite reasonable since the projectile velocity is much larger than the outer-shell electron orbital velocities and hence the Bohr criterion is well satisfied. Moreover, it was found previously that application of this same analysis procedure (including the above assumption) to the determination of the average charges of Xe ions emerging from thin carbon targets yielded average charges that were in good agreement with those determined by magnetic analysis [12]. It should be noted that the L- and M-electron populations and average projectile charges listed in Table I apply only to those ions that emit L x rays (i.e., ions that have lost at least one L electron and retained at least one M electron). In order to estimate the average ionic charges of all the ions, it is necessary to know both the fraction of ions having zero L

electrons and the fraction of ions having zero M electrons. However, corrections to the average charges for these missing fractions are relatively small and tend to cancel each other since inclusion of the zero-L-vacancy fraction will *lower* the average charge by no more than one unit and inclusion of the zero-M-vacancy fraction will *raise* the average charge by no more than one unit.

The average L-shell populations $\bar{n}_L$ listed in Table I for the He, Ne, and Ar targets decrease very slowly with projectile energy and show little dependence on the target atomic number, except at an incident energy of 14.4 MeV/nucleon, where the $\bar{n}_L$ value for He suddenly decreases by 1.5 electrons. The average M-shell populations $\bar{n}_M$, on the other hand, decrease much more rapidly with projectile energy and they display a higher sensitivity to the target species. In general, the L- and M-shell populations obtained in the present analysis of spectra for gas targets are substantially larger than those obtained previously [12,13] for solid targets of comparable (average) atomic number. In the case of $\bar{n}_L$, the gas target values are larger by approximately 0.7 units at an incident projectile energy of 5.2 MeV/nucleon and by 2.7 units at 14.4 MeV/nucleon. The values of $\bar{n}_M$ in gases are approximately 1.8 units larger than those in solids at an incident projectile energy of 5.2 MeV/nucleon, but as the energy increase, $\bar{n}_M$ approaches unity for both target media.

A simple model can be utilized to predict the behavior of the L-electron population. As an ion travels through matter, it occasionally suffers a relatively close collision with an atom of the medium, causing it to lose one of its L electrons. Subsequently, the L vacancy will be filled either by an electron transition from a higher shell (primarily the M shell in the current case) or by capture of an electron to the projectile L shell from an atom of the medium. If the rates of these two processes are large compared to the rate of L-shell ionization, only transitions from ions having single L vacancies will appear in the L x-ray spectrum. Conversely, if the rates for filling an L vacancy are smaller than the rate for producing one, then multiple L vacancies will accumulate in consecutive L-shell ionizing collisions. Within the framework of this simplified picture, the net rate of change of the L-shell population is given by the rate equation

$$\frac{dn_L}{dt}=\lambda_F(N_L-n_L)-\lambda_I n_L, \tag{1}$$

where λ_I is the rate constant for L-shell ionization, λ_F is the rate constant for L-vacancy filling (via capture and decay), and N_L is the number of L shell electrons in a neutral atom (eight). Transformation of the time dependence to a target depth dependence [e.g., $dn_L/dx=(1/v)(dn_L/dt)$, where x is depth and v is projectile velocity] and solution of the resulting differential equation yield

$$n_L=n_L^{\infty}+(N_L-n_L^{\infty})e^{-Ax}, \tag{2}$$

where $A=(\lambda_F+\lambda_I)/v$ and n_L^{∞} is the value of n_L at large depths (i.e., when $x \geq$ the equilibrium thickness). The expression for n_L^{∞} may be written in terms of cross sections

$$n_L^{\infty}=\left(\frac{\sigma_F}{\sigma_F+\sigma_I}\right)N_L. \tag{3}$$

(Cross section is related to rate constant by $\sigma=\lambda/[\eta v]$, where η is the atom density of the target.) With $R=\sigma_F/\sigma_I$, the fractional L-shell population at equilibrium becomes

$$f_L^{\infty}=\frac{n_L^{\infty}}{N_L}=\frac{R}{R+1}. \tag{4}$$

Rate constants for transitions from the M shell to the L shell in Xe range from 2.9×10^{15} s^{-1} for atoms with a single L vacancy and a fully populated M shell [15,16] to approximately 1.7×10^{13} s^{-1} for atoms with a single L vacancy and a single M electron. At a projectile energy of 14.4 MeV/nucleon, conversion of these rate constants into their equivalent cross sections (under the conditions of the gas target measurements) gives values of 2.4×10^{-14} cm^2 and 1.4×10^{-16} cm^2 for a fully occupied M shell and a singly occupied M shell, respectively. Combining these numbers with cross sections for L-shell ionization and capture (estimated using the ECPSSR model [17,18]) yields R values ranging from 1.3×10^6 to 7.4×10^3 for a He target and from 1.9×10^4 to 1.1×10^2 for an Ar target. Hence, this simple model predicts that multiple L-vacancy accumulation should be entirely negligible for all of the gas target cases examined in the present investigation. Experimentally this is true (or nearly so) for all of the spectra obtained at projectile energies below 14.4 MeV/nucleon. The R values predicted for solids are much smaller than for gases due to the higher atom density of the solid state. For example, the estimated R values for a solid KCl target (same average atomic number as Ar) range from 27 (fully occupied M shell) to 0.16 (singly occupied M shell). Therefore, the experimental results obtained from the solid target spectra are quite consistent with the model predictions.

One possible explanation for the observation of higher amounts of multiple ionization than predicted in the spectra obtained with gases at a projectile energy of 14.4 MeV/nucleon is that the ionization of Xe L electrons via collisions with the electrons of the target medium becomes energetically possible above 9.2 MeV/nucleon. However, because the ions have lost many M electrons, the associated L-electron binding-energy increases shift the onset of contributions from this additional ionization mechanism to significantly higher projectile energies. (The energy at which Xe ions with fully stripped M shells achieve the same average velocity as their L-shell electrons is approximately 14.4 MeV/nucleon). While the electron-electron ionization mechanism might account for the small degree of multiple-L-shell ionization observed in the spectra obtained with the Ne and Ar targets, it cannot explain the high relative intensities of x rays from multiple L-vacancy states appearing in the spectrum obtained with a He target. The most likely cause of this unexpected behavior is that at 14.4 MeV/nucleon in He the Xe ions have lost essentially all of their M electrons and, hence, the L vacancies produced in consecutive collisions become ''frozen in'' because there are no decay channels available for filling them and the cross sections for electron capture in He are extremely small. Therefore, the only ions that emit L x rays are the relatively few that happen to pick up an M electron as they pass through the spectrometer observation region.

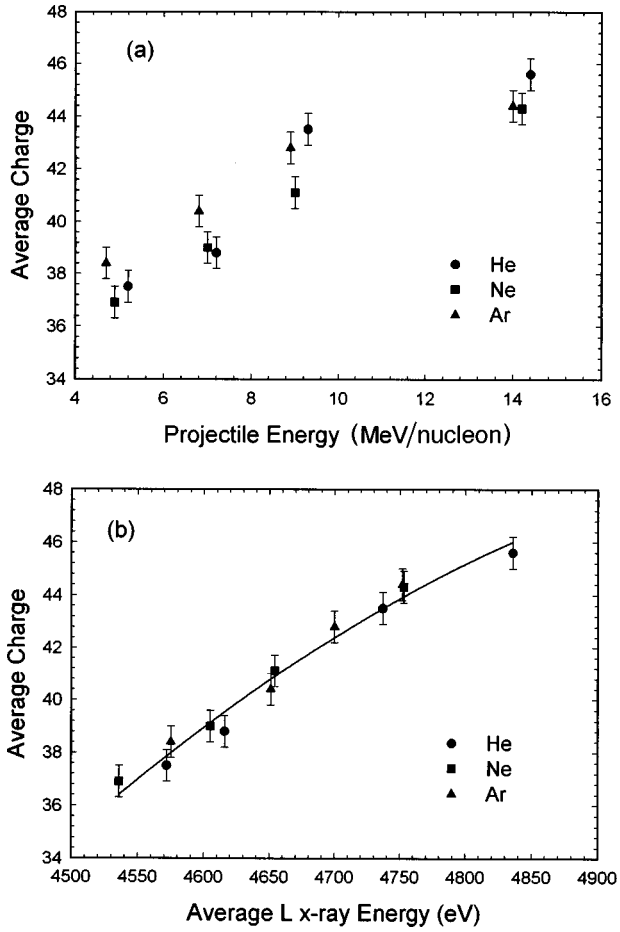

FIG. 5. Average charges of Xe ions that emit L x rays in the indicated gas targets as a function of (a) average projectile energy at the center of the observation region, and (b) average L x-ray energy.

C. Average charges

The average charges determined for Xe ions traveling in He, Ne, and Ar are shown as a function of the average projectile energy at the center of the spectrometer viewing region in Fig. 5(a). As expected from the appearance of the x-ray spectra, there is very little evidence for any significant dependence of the average charge on the atomic number of the target. Figure 5(b) shows the correlation between the average charge and the average L x-ray energy. It is to be expected that the average charge should be closely connected to the average x-ray energy, and the fact that these quantities, which were determined independently, do display a high degree of correlation lends confidence to the reliability of the analysis procedure.

In view of the current state of uncertainty concerning the average charges of fast ions traveling in solids and gases, it is of interest to compare the present charges deduced from the L x-ray spectra of Xe ions in gases with those obtained previously for Xe ions in solids. Unfortunately, as was shown in Ref. [13], low-Z_2 solid targets, such as Li and NaF, are quite transparent to Xe L x rays and, hence, contributions to the spectrum originate from a wide range of depths. This means that the charges deduced from x-ray spectra for low-Z_2 targets have been averaged over a large range of projectile energies. However, in the case of a KCl target, the relatively high absorption coefficients for Xe L x rays greatly limit the depth from which they may be detected. Hence, even a thick KCl target is ''thin'' with respect to the Xe L x-ray spectrum, and so the projectiles that emit detectable x rays in this target are characterized by a small energy loss and a well defined average energy. The average charges determined for Xe ions traveling in solid KCl and gaseous Ar are compared in Fig. 6. It is evident from this figure that the average charge is higher in the solid than in the gas by approximately 2.3 units over the whole range of energies investigated. Bimbot *et al.* [10] have deduced effective charges for 3.5 MeV/nucleon Ne, Ar, Cu, Kr, and Ag ions in a variety of solid and gaseous substances from stopping power measurements. Extrapolation of their results to 3.5 MeV/nucleon Xe ions yields an effective charge in solids that is higher by approximately 1.5 units than that for gases at $Z_2=18$.

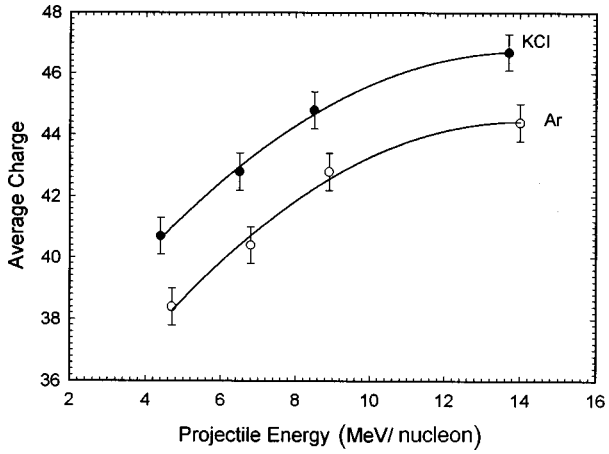

FIG. 6. Average charges of Xe ions that emit L x rays in gaseous Ar and solid KCl as a function of average projectile energy.

The charge distribution widths listed in Table I are comparable to those for ions emerging from solid targets [19]. Also, the value of σ_Q obtained for an Ar target is similar to the value obtained previously for a KCl target.

IV. CONCLUSIONS

The spectra of L x rays emitted by 5.2- to 14.4-MeV/nucleon Xe ions traveling in gas targets of He, Ne, and Ar have been measured. Analysis of the spectra has provided estimates of the average projectile L- and M-electron populations, and the projectile ionic charges inside the gaseous media. It was found that the average number of Xe L electrons decreased only slightly over the projectile energy range from 5.2 to 9.3 MeV/nucleon, while the average number of Xe M electrons decreased quite rapidly. The expected rates for L-vacancy production by ionization, and L-vacancy filling by M-to-L transitions and electron capture to the L shell from the target medium, are consistent with the relatively small contributions of multiple-L-vacancy states observed in the L x-ray spectra obtained for all of the gases in this energy range. However, the increased contributions to the L x-ray spectra from Xe ions having multiple L vacancies observed at 14.4 MeV/nucleon were attributed to the onset of L-shell ionization via electron-electron collisions and the highly stripped condition of the M shell. This latter factor, which causes L vacancies produced in consecutive L-shell ionizing

collisions to become ''frozen in'' when there are no M electrons available for L-vacancy filling transitions, had a dramatic effect on the x-ray spectrum for 14.4 MeV/nucleon Xe ions traveling in He.

Comparison of the present L x-ray spectra for Xe ions traveling in gases with those measured previously for Xe ions traveling in solids having comparable (average) atomic numbers revealed that multiple L-vacancy production is much more probable in solids than in gases. This observation was found to be consistent with the fact that the collision frequency is much larger in the high density environment of a solid than it is in a gas. The estimated ionic charges for Xe ions traveling in gaseous Ar were 2.3 units lower than those determined for Xe ions traveling in solid KCl. This observation confirms conclusions about the average charges of fast heavy ions in gases and solids deduced from stopping power measurements.

ACKNOWLEDGMENTS

This work was supported by the Robert A. Welch Foundation. We thank D. Fry and P. Kottenstette for their assistance with some of the measurements.

[1] N. Bohr and J. Lindhard, K. Dan. Vidensk. Selsk. Mat. Fys. Medd. **28**, 1 (1954).
[2] P. E. Pierce and M. Blann, Phys. Rev. **173**, 390 (1968).
[3] M. D. Brown and C. D. Moak, Phys. Rev. B **6**, 90 (1972).
[4] H. D. Betz and L. Grodzins, Phys. Rev. Lett. **25**, 211 (1970).
[5] S. Datz, B. R. Appleton, J. R. Mowat, R. Laubert, R. S. Peterson, R. S. Thoe, and I. A. Sellin, Phys. Rev. Lett. **33**, 733 (1974).
[6] S. Della-Negra, Y. Le Beyec, B. Monart, K. Standing, and K. Wein, Phys. Rev. Lett. **58**, 17 (1987).
[7] H. Geissel, Y. Laichter, W. F. W. Schneider, and P. Armbruster, Phys. Lett. **88A**, 26 (1982).
[8] H. Geissel, Y. Laichter, W. F. W. Schneider, and P. Armbruster, Phys. Lett. **99A**, 77 (1983).
[9] R. Bimbot, C. Cabot, D. Gardes, H. Gauvin, R. Hingmann, I. Orliange, L. De Reilhac, and F. Hubert, Nucl. Instrum. Methods Phys. Res. B **44**, 1 (1989).
[10] R. Bimbot, C. Cabot, D. Gardes, H. Gauvin, I. Orliange, L. De Reilhac, K. Subotic, and F. Hubert, Nucl. Instrum. Methods Phys. Res. B **44**, 19 (1989).
[11] H. Gauvin, R. Bimbot, J. Herault, B. Kubica, R. Anne, G. Bastin, and F. Hubert, Nucl. Instrum. Methods Phys. Res. B **47**, 339 (1990).
[12] V. Horvat, R. L. Watson, and R. Parameswaran, Phys. Rev. A **51**, 363 (1995).
[13] V. Horvat, R. L. Watson, and J. M. Blackadar, Phys. Rev. A **56**, 1904 (1997).
[14] G. J. Pedrazzini, J. Pálinkás, R. L. Watson, D. A. Church, and R. A. Kenefick, Nucl. Instrum. Methods Phys. Res. B **10/11**, 904 (1985).
[15] E. J. McGuire, Phys. Rev. A **3**, 587 (1971).
[16] J. H. Scofield, At. Data Nucl. Data Tables **14**, 121 (1974).
[17] W. Brandt and G. Lapicki, Phys. Rev. A **23**, 1717 (1981).
[18] G. Lapicki and F. D. McDaniel, Phys. Rev. A **23**, 975 (1981).
[19] R. O. Sayer, Rev. Phys. Appl. **12**, 1543 (1977).